Journal of the European Ceramic Society 15 (1995) 1163–1170

0955-2219(95)00090-9
0955-2219/95/$9.50

Dense Ceramics of $BaTiO_3$ Produced from Powders Prepared by a Chemical Process

C. Miot, C. Proust & E. Husson*

Laboratoire de Physique et Mécanique des Matériaux, ESEM, Université d'Orléans et CRPHT-CNRS, 45071 Orléans Cedex 2, France

(Received 24 January 1995; received in revised form 19 May 1995; accepted 22 May 1995)

Abstract

A sintering optimization of barium titanate ceramics from fine-grained and homogeneous reproducible powders obtained by the citric process is presented. Different sintering parameters are studied: heating rates, final temperature, dwelling times at this final temperature, and influence of the powder deagglomeration step. The sintering is followed by dilatometric measurements. The ceramics obtained by sintering at 1230 or 1300°C are free of barium carbonate, the residual carbon content being estimated at about 400 ppm in the surface layer. They exhibit a grain size close to 1 μm, a structure in which the cubic and tetragonal phases coexist, and a density of about 96% of the theoretical density. Their permittivity and loss factor are respectively about 5000 and 2·5 × 10⁻² at 25°C.

1 Introduction

Barium titanate ceramics are extensively used in the manufacture of ceramic multilayer capacitors. These applications require materials with a good density, a high dielectric constant and a low loss factor. Synthesis of materials with these properties needs fine-grained ceramics, which may be obtained from fine-grained and homogeneous reproducible powders. In a previous paper, we have presented the elaboration of such a powder from a citric resin process.[1] Here is given a sintering optimization study to obtain ceramics with good dielectric properties. The different physical and chemical characteristics of the ceramics obtained were investigated by several methods: dilatometric measurements, X-ray diffraction (XRD), scanning electron microscopy (SEM), thermogravimetric analysis (TGA), infra-red spectroscopy (IR) and nuclear analyses.

2 Experimental Procedure

$BaTiO_3$ powders were obtained from a citric resin method, described in previous papers.[1–3] The mixed citrate $BaTi(C_6H_6O_7)_3.6H_2O$ was first prepared, then dissolved in a citric acid, ethylene glycol and water mixture so that R = ($BaTiO_3$ mass)/(solution mass ratio) was 1%. This solution was calcined at 700°C in static air and $BaTiO_3$ powders were produced after 2 h. Powders elaborated by this method exhibit a Ba/Ti ratio equal to 1. After a careful deagglomeration step,[1] powders were calcined at 700°C for 4 h before being isostatically pressed at 250 MPa in the form of discs and then sintered.

X-ray diffraction patterns of crushed ceramics were obtained using a Siemens D500 diffractometer with the CuK_α wavelength at room temperature. The 400–004 diffraction lines were accurately recorded in the range $98{\cdot}5° < 2\theta < 102{\cdot}5°$ in steps of 0·01° (2θ) with a counting time of 80 s per data point.

Thermogravimetric measurements were made with a Setaram thermobalance under flowing oxygen atmosphere. Approximately 100 mg of ceramic was accurately weighted in a platinum crucible. The temperature was raised from room temperature to 1000°C at 10°C min^{-1} and then from 1000 to 1400°C at 5°C min^{-1}.

FTIR reflection spectra were recorded with a Brucker IFS 113+88 interferometer between 4000 and 400 cm^{-1} at room temperature on a sample containing 2 mg of $BaTiO_3$ dispersed in 200 mg of KBr and pressed into pellets.

The residual carbon concentration was determined by the $^{12}C(d, p)^{13}C$ nuclear technique using deuterons from the CERI's† Van de Graaff generator. The

*To whom correspondence should be addressed.
†CERI. Centre d'Etude sur les Radiations Ionisantes, CNRS Orléans.

method has been described elsewhere.[4–6] The measurements were performed at 950 keV deuteron energy in an ultra-high vacuum chamber under a vacuum of about 10^{-9} mbar obtained with a cryogenic pumping system. The disc samples were sintered ceramics of about 3 mm in thickness and 11 mm in diameter. In the experimental conditions used,[7] taking into account the differential cross-section[8] and the density of the material, the maximal penetration depth is estimated to be about 1 μm and the carbon in the surface layer (about 0·4 μm) may be determined with a precision of 10%.

The SEM images were obtained with a Cambridge stereoscan 100 microscope on the fracture surfaces of samples previously metallized with platinum. The transmission electron microscopy (TEM) images were obtained with a Philips SM20 microscope.

Final densities were evaluated by geometrical measurements and confirmed by: (i) mercury intrusion data (Micrometric 9300 apparatus); (ii) helium pycnometry data (Accupic 1330 apparatus).

Dilatometric measurements were made in a Setaram vertical dilatometer with a constant force load equivalent to 1 g. The derivative curve of shrinkage versus temperature may be calculated electronically. The measurement of the shrinkage, reported for room temperature, allows the estimation of the final density from the green compact one. The value of 6·02 g cm^{-3} was used as the theoretical density, d_{th}.

Dielectric measurements of the ceramics were carried out on an automated Hewlett-Packard impedancemeter HP 4194A. The relative dielectric constant ϵ' and loss factor tg δ were measured between 160 and 120°C at various frequencies (100 Hz, 1 kHz, 10 kHz, 100 kHz and 1 MHz) with a cooling rate of 1°C min^{-1}.

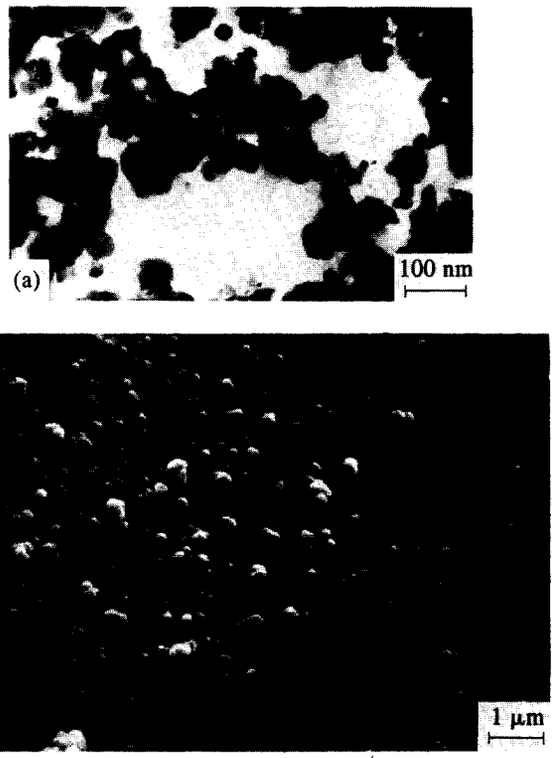

Fig. 1. Microstructure of deagglomerated $BaTiO_3$ powder: (a) 40 nm crystallites observed by TEM; (b) 150 nm spheroide aggregates observed by SEM.

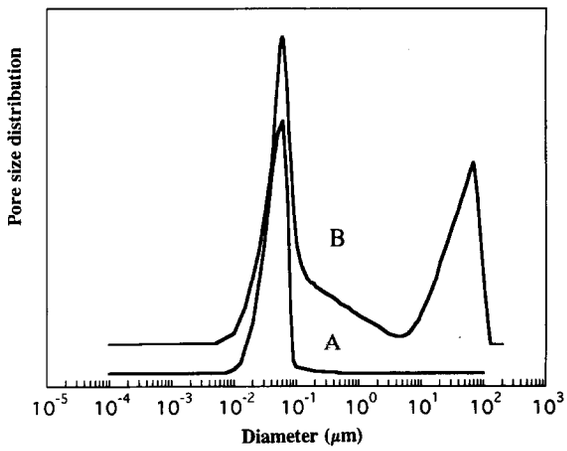

Fig. 2. Pore-size distribution for green compacts of (a) a deagglomerated powder and (b) a raw powder.

3 Results and Discussion

3.1 Raw powders

The sintering behaviour strongly depends on the green states, thus it was very important to know the powder characteristics. The latter were studied and described in detail in a previous paper.[1] Here only the microstructure of the raw deagglomerated powder is given again: it can be described by crystallites associated into 150 nm spheroid aggregates (Fig. 1).

The results obtained by mercury intrusion, for deagglomerated and non-deagglomerated powders are presented in Fig. 2. The curve obtained with a non-deagglomerated powder shows two pore-size distributions centred on 0·05 and 80 μm (Fig. 2(b)) whereas only one peak, centred on 0·05 μm, is observed on the curve obtained with a deagglomerated powder (Fig. 2(a)).

3.2 Sintering optimization

The green compacts were sintered in air at different temperatures up to 1400°C, using various heating rate conditions reported in Table 1. According to our previous studies,[2,3] it appeared that the best sintering temperature to obtain dense ceramics with fine grain size was approximately 1250°C. Thus, for this final temperature of the sintering cycle, different heating rates were

investigated. The sintering conditions, geometrical densities and grain sizes estimated from SEM observations are reported in Table 1. It can be observed that:

(i) a decrease of the heating rate between 1000 and 1250°C induces an increase of the density and grain size;

(ii) for a slow heating rate (4°C h^{-1} between 1000°C and the final temperature), an increase of the final temperature (up to 1300°C) induces an increase of the density and grain size. In this case, the higher the final temperature, the larger the grain size distribution;

(iii) for sintering steps with a final temperature of 1400°C the ceramics showed a classical bimodal grain-size distribution with large grains (100–200 μm) embedded in a fine-grained matrix. This phenomenon was evidenced by several authors[9–12] and the anomalous grain growth occured when samples were heated up to a final temperature greater than 1380°C.

It appeared that to obtain a good density and a small grain size, the final sintering temperature could be reduced to 1230°C with a slow heating rate between 1000 and 1230°C, for example 4°C h^{-1} (Table 1). The best conditions were the following: heating from 20 to 700°C at 350°C h^{-1}, then from 700 to 1000°C at 50°C h^{-1} and finally from 1000 to 1230°C at 4°C h^{-1}. These sintering conditions will be called '1230°C sintering' in the following text. The ceramics had a geometrical density greater than 96% of d_{th}, and an average grain size of 1·6 μm with 80% of the grains between 0·25 and 2·5 μm size (Fig. 3(a)). At this final temperature, the anomalous grain growth was inhibited.

With these optimized sintering conditions, the effect of the deagglomeration step was studied by sintering a green compact made with a non-deagglomerated raw powder. The resulting ceramics were not densified (61·5% of d_{th}) and showed two grain-size distributions, the first one centred on 0·3 μm and the second one on 2 μm (Fig. 3(b)). A high density (99% of d_{th}) might be obtained by sintering for 2 h at 1400°C; then the grain size was homogeneous but with grains of 100–200 μm size.

Table 1. Sintering conditions investigated around the final temperature of 1230°C. Density (in d_{th} %) and average grain size

Final sintering temperature (°C)	*Sintering rates*	*% d_{th}*	*Grain size (μm)*
1250	20–700 at 350°C h^{-1} 700–1250 at 100°C h^{-1}	92	0·6
1250	20–700 at 350°C h^{-1} 700–1000 at 50°C h^{-1} 1000–1250 at 10°C h^{-1}	95	1·4
1250	20–700 at 350°C h^{-1} 700–1000 at 50°C h^{-1} 1000–1250 at 5°C h^{-1}	95·5	1·8
1260	20–700 at 350°C h^{-1} 700–1000 at 50°C h^{-1} 1000–1260 at 5°C h^{-1}	96	3·2
1300	20–700 at 350°C h^{-1} 700–1000 at 50°C h^{-1} 1000–1300 at 4°C h^{-1}	96	4
1400	20–700 at 350°C h^{-1} 700–1000 at 50°C h^{-1} 1000–1400 at 4°C h^{-1}	95·5	~50 + 3
1230	20–700 at 350°C h^{-1} 700–1000 at 50°C h^{-1} 1000–1230 at 25°C h^{-1}	93	1
1230	**20–700 at 350°C h^{-1} 700–1000 at 50°C h^{-1} 1000–1230 at 4°C h^{-1}**	**96**	**1·6**
1230	20–700 at 350°C h^{-1} 700–1000 at 50°C h^{-1} 1000–1230 at 3°C h^{-1}	95	1·6
1230 (with a non-deagglomerated powder)	20–700 at 350°C h^{-1} 700–1000 at 50°C h^{-1} 1000–1250 at 4°C h^{-1}	61·5	~2 + 0·3

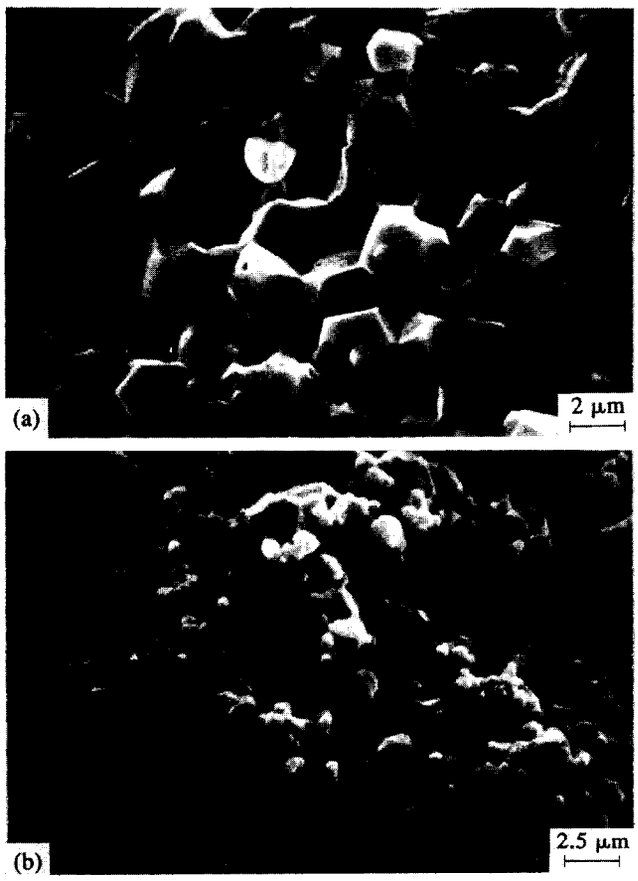

Fig. 3. Microstructure of $BaTiO_3$ ceramics sintered at 1230°C from (a) a deagglomerated powder and (b) a raw powder.

Our results are in good agreement with those of Hiesh and Fang,[12] who showed that:
(i) to obtain a high density and a uniform fine-grained microstructure, a uniform green compact with fine particles was needed;
(ii) it was possible to prepare dense ceramics from non-uniform green compacts but a higher sintering temperature should be used and the ceramics obtained exhibited a large grain size.

To minimize the sintering time it is possible to increase the final sintering temperature to 1300°C. We have followed the procedure previously described and investigated different heating rates. The results are reported in Table 2. It is important to note that an increase of the heating rate from 25 to 350°C h^{-1} between 700 and 1300°C induces a slight decrease of the density and a more sensible decrease of the grain size. This phenomenon was previously observed with the 1230°C sintering. Thus the thermal cycle chosen was the following: heating from 20 to 700°C at 350°C h^{-1} and from 700 to 1300°C at 200°C h^{-1}. The microstructure of the obtained ceramic exhibited an average fine grain size of 0·7 μm with 80% of the grains between 0·25 and 1 μm size (Fig. 4(a)). These sintering conditions will be called '1300°C sintering' in the text below.

Table 2. Sintering conditions with 1300°C final temperature. Density (in d_{th} %) and average grain size

Sintering rates	% d_{th}	*Grain size (μm)*
20–700°C at 350°C h^{-1} 700–1000°C at 50°C h^{-1} 1000–1300°C at 25°C h^{-1}	96	3·8
20–700°C at 350°C h^{-1} 700-1000°C at 50°C h^{-1} 1000–1300°C at 50°C h^{-1}	96·3	1·4
20–700°C at 350°C h^{-1} 700–1300°C at 100°C h^{-1}	94·4	0·8
20–700°C at 350°C h^{-1} 700–1300°C at 200°C h^{-1}	**94·5**	**0·7**
20–1300°C at 350°C h^{-1}	93	0·6

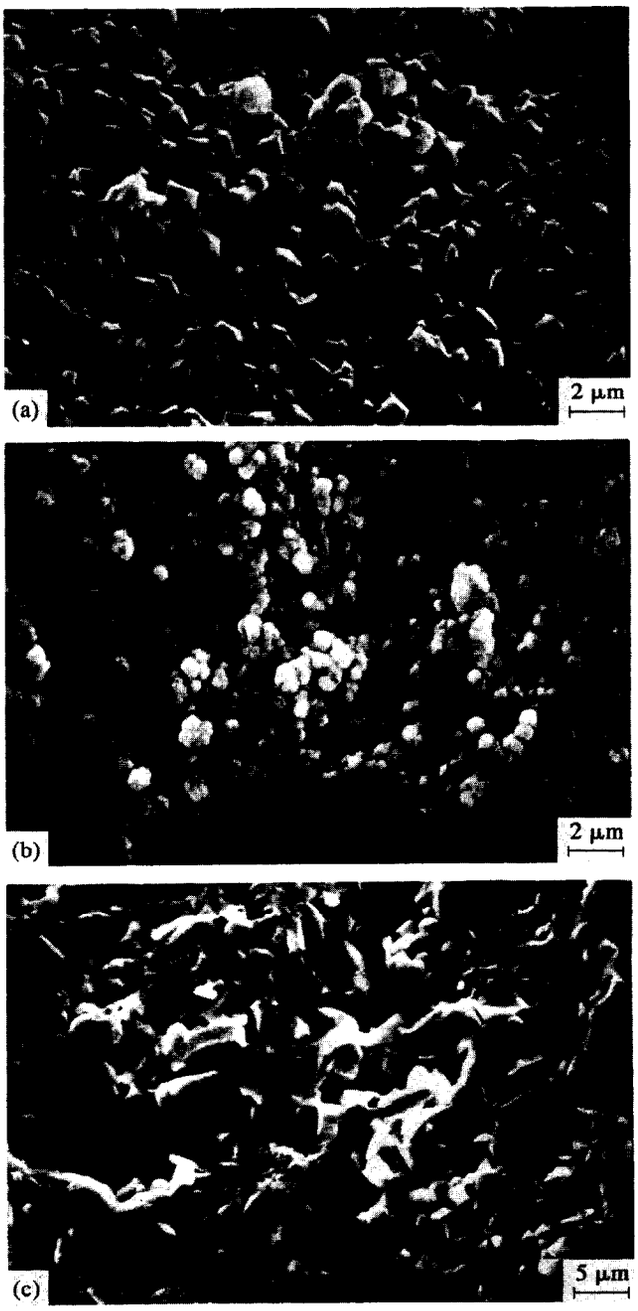

Fig. 4. Microstructure of $BaTiO_3$ ceramics sintered at 1300°C from (a) a deagglomerated powder, (b) a raw powder and (c) a raw powder after a dwelling time of 20 h.

Table 3. Characteristics of the ceramics obtained with deagglomerated powders and sintered at 1300°C versus the dwelling time at this temperature

Dwelling time	*% d_{th}*	*Grain size (μm)*
15 min	95·4	1·03
20 min	95·4	1·05
30 min	95·6	1·50
1 h	95·7	2·10
5 h	95·9	2·70
10 h	96·7	5·65
20 h	96·7	6·10

Table 4. Characteristics of the ceramics obtained with non-deagglomerated powders and sintered at 1300°C versus the dwelling time at this temperature

Dwelling time(h)	*% d_{th}*
0	72·7
1	85
4	85·2
10	85·6
20	86

On the other hand, the influence of the dwelling time was investigated and the results are reported in Table 3. It appears that an increase of the dwelling time has a weak effect on the final density but modifies the grain size and the grain size distribution. The longer the dwelling time, the larger the grain size and its distribution.

The sintering of green compacts made with a non-deagglomerated raw powder in the 1300°C sintering conditions yielded a final density of about 72% of d_{th} (Fig. 4(b)). After holds at 1300°C for different dwelling times, the final density increased up to 86% of d_{th}, after 20 h (Table 4). The ceramics showed anomalous grain growth, the amount of the biggest grains depending on the dwelling time (Fig. 4(c)).

Our results show the importance of a careful deagglomeration step in the elaboration of a sinterable powder. The homogeneity of the powder allows us to obtain both a good density and a well controlled grain size in the ceramics. The double optimized synthesis processes give ceramics with a narrow grain-size distribution centred on 1·6 μm (1230°C sintering) and 0·7 μm (1300°C sintering).

3.3 Characterization of optimized ceramics

Ceramics obtained with 1230 and 1300°C sintering conditions were analysed by different techniques. The IR reflectivity spectra recorded at room temperature did not reveal any trace of barium carbonate in both cases. TGA measurements did not allow us to detect any significant weight loss. Thus, another more sensitive technique was necessary to determine the residual carbon content in these two ceramics. The $^{12}C(d, p)^{13}C$ nuclear technique was used. For ceramics respectively sintered at 1230 and 1300°C, it gave carbon contents of 95 and 130 mg cm^{-2} in the surface layer (0·4 μm). The carbon content is higher in the ceramics obtained by the 1300°C sintering. This result can be explained as follows:

(i) if the residual carbon is assumed to be located at the grain boundaries, it is more important in the finer grain size ceramic;

(ii) during the 1230°C sintering thermal cycle, the treatment time in the furnace was much longer (about 83 h) than during the 1300°C sintering (8 h). Thus the diffusion of carbon from the bulk to the surface layer and then to the atmosphere is facilited, so the detected carbon content is weaker.

The sintering behaviour of the deagglomerated powder was studied by dilatometric measurements in the conditions of pressing (250 MPa) and heating rates of both the 1230 and 1300°C optimized sintering. The obtained shrinkage curves and their derivatives versus temperature are reported in Fig. 5. The derivative curve of the shrinkage versus temperature obtained at 1230°C with a very slow heating rate between 700 and 1230°C, exhibits two minima at about 1060 and 1200°C. Previous studies[2] carried out on the same powders sintered with a constant rate of 150°C h^{-1} showed only one minimum at 1060°C on the derivative curve. Only the difference in heating rate between the two experiments can explain the appearance of a second

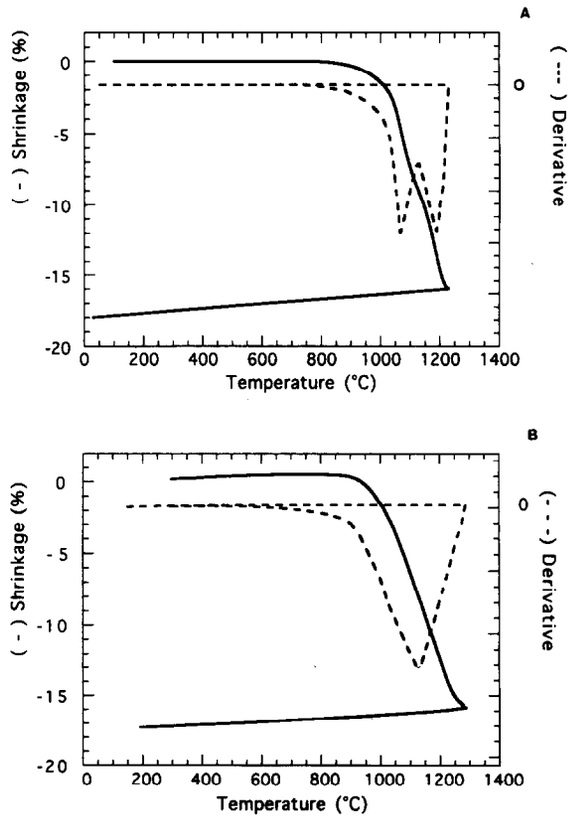

Fig. 5. Dilatometric curves obtained from $BaTiO_3$ ceramics sintered at (a) 1230°C and (b) 1300°C.

Table 5. Measurements of final densities (in %) of ceramics sintered at 1230 and 1300°C

Technique	*1230°C (%)*	*1300°C (%)*
Helium picnometry	98·3	97
Mercury intrusion	97·6	96·2
Shrinkage measurement	98·7	97·1
Geometrical measurement	96	94·5
Average value	97·7	96·2

minimum on the derivative curve in Fig. 5(a). This second minimum was observed only for very slow heating rates during the shrinkage. On the contrary, the shrinkage derivative curve obtained in the 1300°C sintering conditions exhibits only one minimum at 1130°C (Fig. 5(b)). The temperature of the minimum is shifted towards the high temperatures due to the faster heating rate (300 then 200°C h^{-1} instead of 150°C h^{-1} in Ref. 2). The shrinkage measurement reported at room temperature gives a value of the ceramic density. The final density of the two types of ceramic determined by different methods are given in Table 5. They are in very good agreement with the values deduced from shrinkage measurements. In both cases the final densities are satisfactory since they are greater than 96% of d_{th}.

X-ray diffraction patterns of the two ceramics are characteristic of a mixture of tetragonal and cubic phases. The 004–400 diffraction lines accu-

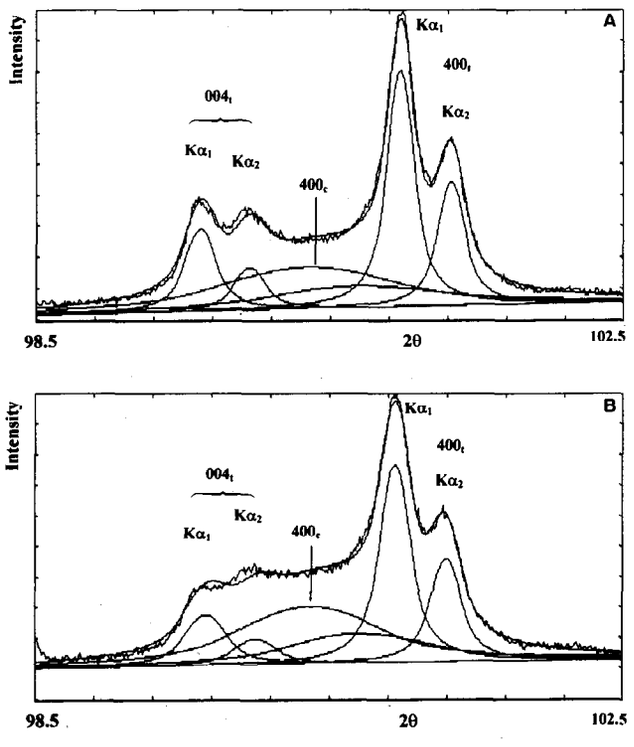

Fig. 6. X-ray diffraction patterns of the 400/004 lines and fits performed with pseudo-Voigt functions for (a) a 1230°C sintered ceramic and (b) a 1300°C sintered ceramic.

Table 6. Tetragonal (t) and cubic (c) phase ratio; average particle size (d) and thickness of the surface cubic phase (l) in the grains for the ceramics sintered at 1230 and 1300°C

	t/c	d(*μm*)	l(*μm*)	*% of cubic phase*
1230°C	1·08	1·6	0·24	52
1300°C	0·76	0·7	0·15	79

rately recorded were fitted with pseudo-Voigt functions. The integrated intensities of the fitted peaks (Fig. 6) allowed us to estimate roughly the relative amounts of the two phases. Three lines were observed: for the 1300°C sintered ceramic the lines at $2\theta = 99{\cdot}64°$ and $100{\cdot}95°$ correspond respectively to the 004 and 400 reflections in the tetragonal phase and the line at $2\theta = 100{\cdot}34°$ corresponds to the 400 reflection in the cubic phase; for the 1230°C sintered ceramic the cubic component is observed at the same diffraction angle whereas the 004 and 400 tetragonal reflections are observed at slightly different angles, $2\theta = 99{\cdot}61°$ and $2\theta = 100{\cdot}98°$, respectively. The results obtained from the integrated intensities giving the fraction of the tetragonal over the cubic phases (t/c) are listed in Table 6, as are the average particle diameters deduced from SEM photogaphs and TEM observations. From results published by Niepce[13] and Takeuchi *et al.*,[14] the thickness of the cubic phase located at the surface of a tetragonal $BaTiO_3$ grain can be estimated by a simple calculation from the t/c ratio[14] using the expression:

$$\frac{t}{c} = \frac{\frac{4}{3}\pi\left(\frac{d}{2} - l\right)^3}{\frac{4}{3}\pi\left(\frac{d}{2}\right)^3 - \frac{4}{3}\pi\left(\frac{d}{2} - l\right)^3}$$

where d is the ceramic grain size and l is the thickness of the cubic layer on the grain surface.

This expression is reduced to: $t/c \approx d/6l$ since $d >> 1$.

Results are in good agreement with those of Niepce[13,15] and Arlt:[16]

(i) at room temperature the presence of coexisting cubic and tetragonal phases in one particle is confirmed;

(ii) the amount of the cubic phase increases with the decrease of the ceramic grain size. Niepce and Arlt indicated that for a ceramic with grain size below 0·7μm, the cubic phase was obtained. In our case the cubic phase was mainly obtained in the ceramic exhibiting an average grain size of 0·7 μm. In the ceramic exhibiting an average grain size of 1·6 μm, the amount of the cubic phase is lower.

Figure 7 shows the temperature dependence of the relative dielectric constant versus temperature at several frequencies for the two optimized

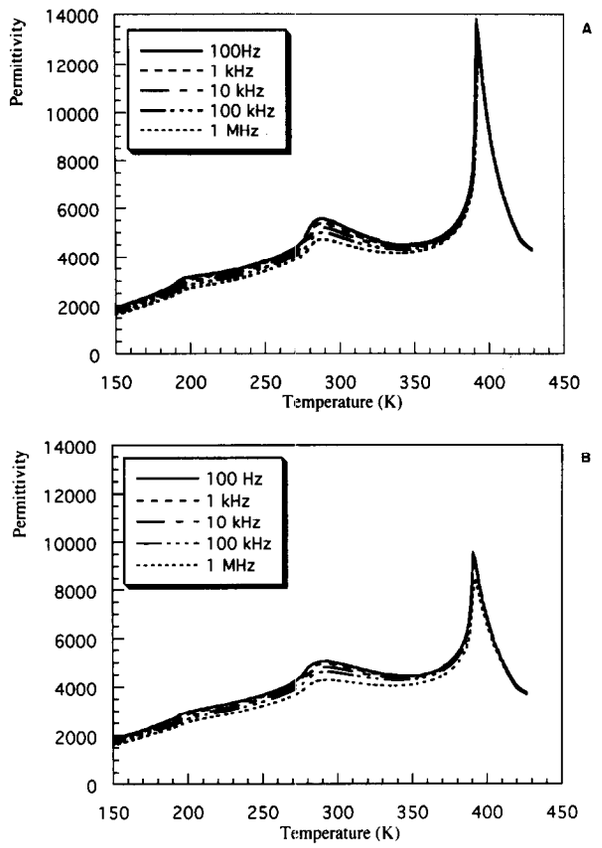

Fig. 7. Permittivity of $BaTiO_3$ ceramics sintered at (a) 1230°C and (b) 1300°C versus temperature at different measurement frequencies.

ceramics. The values of the relative dielectric constant ϵ' and loss factor tg δ at room temperature and at the ferroelectric transition, as well as the T_c temperatures, are reported in Table 7. We can observe that:

(i) the values of the permittivity obtained on the two ceramics depend on the grain size. These results confirm those of Niepce,[13] who showed that at room temperature the permittivity depends on the grain size and exhibits a maximum value for a grain size approximately equal to 0·8 μm;

(ii) the temperature of the phase transition increases with the grain size. This phenomenon was well known and described by several authors;[17–19]

(iii) the value of the permittivity at the ferroelectric transition is higher for a 1·6 μm grain size ceramic than for a 0·7 μm grain size one. This could be related to the amount of the cubic phase present in the latter ceramic which is not concerned by the ferroelectric transition.

Table 7. Dielectric characteristics of the ceramics

Grain size (μm)	*T_c(°C)*	*ϵ max*	*ϵ at 25°C*	*tg δ at 25°C*
1·6	120	13 000	5200	0·025
0·7	118	9 300	4900	0·03

4 Conclusions

The results obtained in this study may be summarized as follows.

(i) It is possible to obtain homogeneous fine-grained $BaTiO_3$ ceramics at quite low temperatures from powders elaborated by a resin citric process.

(ii) To avoid an anomalous grain growth and/or a bimodal grain-size distribution, a careful deagglomeration step of the raw powders is required.

(iii) Two sintering thermal cycles have been proposed to obtain ceramics with a density greater than 96% of d_{th} and a well-controlled grain size: a sintering cycle at 1230°C gave 1·6 μm grain size ceramics and a sintering cycle at 1300°C gave 0·7 μm grain size ceramics. In both cases a narrow grain size distribution was observed.

(iv) The ceramics obtained are free of barium carbonate, the residual carbon content has been estimated at about 400 ppm in the surface layer of the ceramics.

(v) The ceramics exhibit good dielectric characteristics in accordance with previous papers showing that, in $BaTiO_3$ ceramics, higher permittivity as well as low dielectric losses are obtained at room temperature for a grain size of about 0·8 μm.[13]

References

1. Proust, C., Miot, C. & Husson, E., Characterization of $BaTiO_3$ powder obtained by a chemical route. *J. Eur. Ceram. Soc.*, submitted.
2. Coutures, J. P., Odier, P. & Proust, C., Barium titanate formation by organic resins formed with mixed citrate. *J. Mater. Sci.*, **27** (1992) 1849–56.
3. Le Calvé-Proust, C., Husson, E., Odier, P. & Coutures, J. P., Sintering ability of $BaTiO_3$ powders elaborated by citric process. *J. Eur. Ceram. Soc.*, **12** (1993), 153–7.
4. Wengeler, H., Knobel, R., Kathrein, H., Freund, F., Demortier, G. & Wolf, G., Atomic carbon in magnesium oxide single crystals. Depth profiling, temperature- and time-dependent behavior. *J. Phys. Chem. Solids*, **43** (1982) 59–71.
5. Oberheuser, G., Kathrein, H., Demortier, G., Gouska, H. & Freund, F., Carbon in olivine single crystals analyzed by the $^{12}C(d,p)^{13}C$ method and by photoelectron spectroscopy. *Geochimica Cosmochimica Acta*, **47** (1983) 1117–29.
6. Mathez, E. A., Carbon abundances in mantle minerals determined by nuclear reaction analysis. *Geophys. Res. Lett.*, **11** (1984) 947–50.
7. Proust, C., Husson, E.,. Blondiaux, G. & Coutures, J. P., Residual carbon detection in barium titanate ceramics by nuclear reaction technique. *J. Eur. Ceram. Soc.*, in press.
8. Huez, M., Qualia, L. & Weber, G., Fonction d'excitation de la reaction $^{12}C(d,p)^{13}C$ entre 400 et 1350 keV. Distributions angulaires. *Nuclear Instr. Meth.*, **105** (1972) 197–203.

9. Lavielle, D., Poumarat, J., Montardi, Y., Bernard P. & Aguerre-Charriol, O., Microstructure/propriety relationship in chemically processed barium titanate for X7R characteristics. *Euroceramics II*, **3** (1991) 1903–7.
10. Demartin, M., Pethybridge, G. & Carry, C., Sintering, grain growth and de-sintering process in un-doped $BaTiO_3$. *Euroceramics III*, **1** (1993) 787–92.
11. Chen, J., Jin, W. & Yao, Y., Study of the anomalous grain growth of $BaTiO_3$ ceramics. *Ferroelectrics*, **142** (1993) 153–9.
12. Hiesh, H. L. & Fang, T. T., Effect of green states on sintering behavior and microstructural evolution of high-purity barium titanate. *J. Am Ceram. Soc.*, **73** (1990) 1566–73.
13. Niepce, J. C., Permittivity of fine grained $BaTiO_3$. *Electroceramics IV*, **1** (1994) 29–39.
14. Takeuchi, T., Ado, K., Asai, T., Kageyama, H., Saito, Y., Masquelier, C. & Nakamura O., Thickness of the cubic phase on barium titanate single-crystalline grains. *J. Am. Ceram. Soc.*, **77** (1994) 1665–8.
15. Caboche, G., Chaput, F., Boilot, J. P. & Niepce, J. C., Titanate de baryum à grains fins pour application diélectrique. *Silicates Industriels*, **5–6** (1993) 103–7.
16. Arlt, G., The influence of microstructure on the properties of the ferroelectric ceramics. *Ferroelectrics*, **104** (1990) 217–27.
17. Kinoshita, K. & Yamayi, A., Grain-size effects on dielectric properties in barium titanate ceramics. *J. Appl. Phys.*, **47** (1976) 371–3.
18. Fang, T. T., Hiesh, H. L. & Shiau, F. S., Effects of pore morphology and grain size on the dielectric properties and tetragonal-cubic phase transition of high-purity barium titanate. *J. Am. Ceram. Soc.*, **76** (1993) 205–11.
19. Wu, K. & Schulze, W. A., Aging of the weak-field dielectric response in fine- and coarse-grain ceramic $BaTiO_3$. *J. Am. Ceram. Soc.*, **75** (1992) 3390–5.